© 2020. Published by The Company of Biologists Ltd | Journal of Experimental Biology (2020) 223, jeb235705. doi:10.1242/jeb.235705

SHORT COMMUNICATION

A direct excitatory action of lactate ions in the central respiratory network of bullfrogs, *Lithobates catesbeianus*

Michael T. Burton and Joseph M. Santin*

ABSTRACT

Chemoreceptors that detect O_2 and CO_2/pH regulate ventilation. However, recent work shows that lactate ions activate arterial chemoreceptors independent of pH to stimulate breathing. Although lactate rises in the central nervous system (CNS) during metabolic challenges, the ability of lactate ions to enhance ventilation by directly targeting the central respiratory network remains unclear. To address this possibility, we isolated the amphibian brainstem–spinal cord and found that small increases in CNS lactate stimulate motor output that causes breathing. In addition, lactate potentiated the excitatory postsynaptic strength of respiratory motor neurons, thereby coupling central lactate to the excitatory drive of neurons that trigger muscle contraction. Lactate did not affect motor output through pH or pyruvate metabolism, arguing for sensitivity to lactate anions per se. In sum, these results introduce a mechanism whereby lactate ions in the CNS match respiratory motor output to metabolic demands.

KEY WORDS: Control of breathing, Lactate, Motor circuit, Motor neuron, Ventilation

INTRODUCTION

The regulation of breathing is fundamental for metabolic and acid–base homeostasis in animals. The classic model for breathing control in vertebrates is as follows: chemoreceptors in the brain and peripheral arterial blood sense levels of CO_2/pH and O_2, respectively. When these gases are disturbed from their regulated values, chemosensors detect the change and then modify activity of the brainstem respiratory network to elicit ventilatory compensation (Guyenet and Bayliss, 2015). Accordingly, much work has sought to understand how CO_2/pH and O_2 are sensed, and metabolites such as ATP (Cinelli et al., 2017; Gourine et al., 2010; Rajani et al., 2018) and lactate ions (Chang et al., 2015) have emerging roles in the transduction of these gases for the control of breathing.

Of interest is the lactate ion as a regulator of peripheral chemoreceptor function and O_2 homeostasis. Early studies found that increases in arterial lactate ions enhance ventilation independent of pH (Hardarson et al., 1998) and that the hypoxic ventilatory response involves lactate production (Gargaglioni et al., 2003). Recently, the primary O_2 sensor in mammals, the carotid body, was shown to express a G-protein coupled receptor (Olfr78) that can bind lactate, which may (Chang et al., 2015) or may not (Chang et al., 2018; Peng et al., 2020; Torres-Torrelo et al., 2018) transduce lactate to increase ventilation during hypoxia. Regardless of controversy over mechanisms, the potential role of lactate in ventilatory control appears to be conserved across vertebrates, as increases in arterial lactate stimulate ventilation in fishes, fish gills express putative lactate ion receptors, and denervation of the first gill arch, which carries sensory feedback to the brainstem, reduces ventilatory sensitivity to lactate (Thomsen et al., 2019; Thomsen et al., 2017). Although peripheral lactate sensitivity has received considerable attention, it remains unknown whether lactate targets sites other than peripheral chemoreceptors to control ventilation.

We propose that lactate ions may regulate breathing through mechanisms in the central respiratory network for the following reasons. First, lactate rises in the central nervous system (CNS) during hypoxia and exercise (e.g. Bisgard et al., 1978; Matsui et al., 2017), which could present the respiratory network with a lactate signal to alter ventilation. Second, peripheral chemoreceptor denervation reduces, but does not eliminate, ventilatory responses to arterial lactate (Thomsen et al., 2019, 2017), suggesting that other sites may contribute to ventilatory control by lactate ions. Finally, lactate ions cross the blood–brain barrier (Bergersen, 2015); thus, experiments showing that arterial blood lactate stimulates ventilation do not rule out a possible contribution from central sensory mechanisms. On this background, we tested the hypothesis that lactate ions stimulate the central respiratory network. The isolated brainstem–spinal cord preparation of the American bullfrog, *Lithobates catesbeianus* (Shaw 1802), is well suited to test this hypothesis because it produces respiratory motor patterns closely resembling those observed *in vivo* (Baghdadwala et al., 2016), allowing us to unambiguously test for central actions of lactate. To this end, we examined (1) whether the central respiratory network responds to lactate, (2) whether lactate sensitivity relates to pH, metabolism or the lactate anion per se, and (3) which cell types lactate targets.

MATERIALS AND METHODS

Ethical approval

All experiments were approved by the Institutional Animal Care and Use Committee at The University of North Carolina at Greensboro.

Animals

Adult female American bullfrogs (*L. catesbieansus*; n=32; body mass ~100 g) were purchased from Rana Ranch (Twin Falls, ID, USA). Bullfrogs were housed in plastic tanks in aerated, dechlorinated tap water at 22°C and fed pellets provided by Rana Ranch twice per week. Frogs had access to both wet and dry areas in tanks.

Brainstem–spinal cord preparation

To generate the rhythmic brainstem–spinal cord preparation, frogs were deeply anesthetized with ~1 ml of isoflurane in a sealed box (~500 ml) until a toe-pinch fail to produce movement and then were rapidly decapitated. The head was immersed in 4°C artificial cerebrospinal fluid (aCSF) containing (in mmol l^{-1}): 104 NaCl, 4 KCl, 1.4 $MgCl_2$, 7.5 D-glucose, 40 $NaHCO_3$, 2.5 $CaCl_2$ and 1

The University of North Carolina at Greensboro, Department of Biology, Greensboro, NC 27412, USA.

*Author for correspondence (jmsantin@uncg.edu)

J.M.S., 0000-0003-1308-623X

Received 15 August 2020; Accepted 3 November 2020

NaH_2PO_4, gassed with 1.5% CO_2/98.5% O_2 (pH 7.85). The skull covering the brainstem and forebrain was removed within about 10 min, the animal was decerebrated, and then the brainstem–spinal cord was removed, ensuring the nerves remained undamaged. The dura covering the brainstem and spinal cord was then removed. The spinal cord was transected caudal to the hypoglossal nerve and the brainstem–spinal cord was then pinned ventral side up in a 6 ml Sylgard-coated Petri dish. aCSF bubbled with 1.5% CO_2/98.5% O_2 was circulated through the Petri dish with a peristaltic pump at ∼7 ml min^{-1} (Mini Pump Variable Flow, Fisher Scientific, Hampton, NH, USA) at 20°C for about 4 h before experiments. Hyperoxia was chosen to increase the driving force for O_2 diffusion into the tissue, and 1.5% CO_2 was chosen because this approximates the physiological CO_2 level for these animals.

Extracellular nerve recordings

All preparations produced fictive respiratory burst activity throughout the experimental procedures. Respiratory-related extracellular nerve activity was recorded from the hypoglossal nerve (HG) and cranial X (CN X; the vagus nerve). Glass electrodes were made from borosilicate glass pulled to a fine tip using a P87 horizontal pipette puller (Sutter Instruments, Novato, CA, USA). Glass pipettes were broken to fit snuggly around the nerve roots and then fire polished. HG and CN X were pulled into the glass pipette using syringes attached the suction electrodes. Extracellular activity of nerve roots was amplified (×1000), filtered (low pass, 1000; high pass,100) using an AM-Systems 1700 amplifier (Sequim, WA, USA), digitized with a Powerlab 8/35 (ADInstruments, Sydney, NSW, Australia), and rectified and integrated (100 ms τ) using the LabChart data acquisition system (ADInstruments).

Motor neuron labeling and whole-cell patch clamp electrophysiology

Brainstem–spinal cords were dissected as described above. HG neuron cell bodies were labeled by backfilling motor axons with ∼1 µl of 10% tetramethylrhodamine dextran (TRITC dextran) for 1 h and 45 min as previously described (Santin et al., 2017). This was enough time to observe robust labeling in the region of the HG motor nucleus that lies rostral to the obex, thought to be homologous to the mammalian hypoglossal nucleus. This region was selected because it mostly contains cell bodies that innervate the hyoglossus and geniohyoid (Takei et al., 1987), muscles that are involved in generating the inspiratory powerstroke in *L. catesbeianus* (Sakakibara, 1983a). After the backfilling procedure, the brainstem–spinal cord was glued to an agar block dorsal-side out, submerged in cold aCSF, and cut into 300 µm thick slices with a vibrating microtome. Slices were allowed to recover for at least 1 h in aCSF at room temperature before recordings.

Slices were then placed in the ∼0.5 ml recording chamber on a fixed-stage microscope (FN1, Nikon Instruments Inc., NY, USA) for whole-cell patch clamp recording of labeled motor neurons. The slice was superfused with aCSF bubbled with 98.5% O_2/balance CO_2, supplied by a gravity-fed system at a rate of ∼2 ml min^{-1}. The region of interest containing TRITC-dextran labeled neurons was imaged at 4× magnification, and then individual neurons were located in the slice at 60× magnification (excitation, 540 nm: emission, 605 nm). Real-time imaging was performed with a Hamamatsu ORCA Flash 4.0LT sCMOS Camera (Hamamatsu Photonics, Hamamatsu City, Japan). Once a labeled neuron was identified, the cell was approached by the whole-cell patch pipette controlled by a Sutter Instrument micromanipulator system that included a MP-285 micromanipulator and a MPC-200 controller (Sutter Instrument, Novato, CA, USA). Whole-cell patch pipettes were pulled with a P87 horizontal pipette puller (Sutter Instrument) and had resistances of 3–4 MΩ when filled with the following solution (in mmol l^{-1}): 110 potassium gluconate, 2 $MgCl_2$, 10 Hepes, 1 Na_2-ATP, 0.1 Na_2-GTP and 2.5 EGTA. The cell of interest was approached with slight positive pressure on the pipette. When an indentation could be seen on the cell in the bright field with IR-DIC optics, positive pressure was removed and a >1 GΩ seal was formed by applying slight negative pressure through the pipette by mouth. Whole-cell access was obtained by rapid negative pressure applied by mouth to rupture the gigaohm seal. Cells were then allowed ∼3–5 min for series resistance to stabilize. Series resistance was not compensated and did not vary throughout the experiment (time control neurons in aCSF: 9.03±1.6 MΩ at the beginning of the experiment and 10.01±1.9 MΩ at the end; sodium lactate-exposed neurons: 9.5±1.6 MΩ at the beginning of the experiment and 9.9±0.7 MΩ at the end; means±s.d.). Experiments where series resistance varied by >20% were discarded.

Experimental procedures

Series 1: neural respiratory response to lactate

Preparations (n=7) were allowed to recover for about 4 h before exposure to lactate ions (Lac^-). Nerve activity in all preparations (amplitude and frequency) had stabilized for at least 30 min before Lac^- exposure. Once preparations had stabilized, 1 mmol l^{-1} sodium lactate dissolved in aCSF was superfused across the preparation for 1 h and then washed with control aCSF until burst amplitude returned to baseline. To determine whether these responses were repeatable within the same preparation, n=2 preparations in this group were exposed to 1 mmol l^{-1} sodium lactate for a second time after recovery back to baseline (e.g. Fig. 1B). In these two preparations, HG burst amplitude in response to Lac^- increased during the two exposures to a similar extent (preparation 1: exposure 1, 63%; exposure 2, 57% over baseline; preparation 2: exposure 1, 27%; exposure 2, 22% over baseline). Solutions were continuously gassed with 1.5% CO_2/98.5% O_2. The pH of the aCSF was 7.77 and the pH of 1 mmol l^{-1} sodium lactate was 7.81.

Series 2: dose–response to lactate, HCO_3^- and pyruvate

In these experiments, rhythmic preparations were allowed to recover for about 4 h before exposure to the treatments. All preparations had stable activity for at least 30 min before exposure to the treatment conditions. Preparations were then sequentially superfused with 0.5, 2 and 4 mmol l^{-1} of sodium lactate (Lac^-), sodium bicarbonate (HCO_3^-) and sodium pyruvate (Pyr^-) for 20 min at each concentration. Solutions were continuously gassed with 1.5% CO_2/98.5% O_2. The pH of the aCSF for each concentration (0.5, 2 and 4 mmol l^{-1}) for the chemicals was as follows: Lac^- 7.80–7.85, HCO_3^- 7.8–7.85, Pyr^- 7.77–7.81. We acknowledge the pH was changing during these experiments; however, the pH changes of the bathing solution over this range of concentrations was small.

Series 3: whole-cell patch clamp electrophysiology

Membrane potential, firing frequency, input resistance, series resistance and spontaneous excitatory postsynaptic currents (sEPSCs) of single motor neurons were measured before and after 25 min of either no treatment (time control) or 2 mmol l^{-1} sodium lactate dissolved in aCSF. As these neurons are normally rhythmically active *in vivo*, neurons were pulsed with current (∼2.5× rheobase) for 1.5 s, 10 times per minute to simulate typical rhythmic activation of hypoglossal motor neurons *in vivo* (Kogo and Remmers, 1994). We chose this approach because neurons would never be exposed to lactate without suprathreshold rhythmic

Journal of Experimental Biology (2020) 223, jeb235705. doi:10.1242/jeb.235705

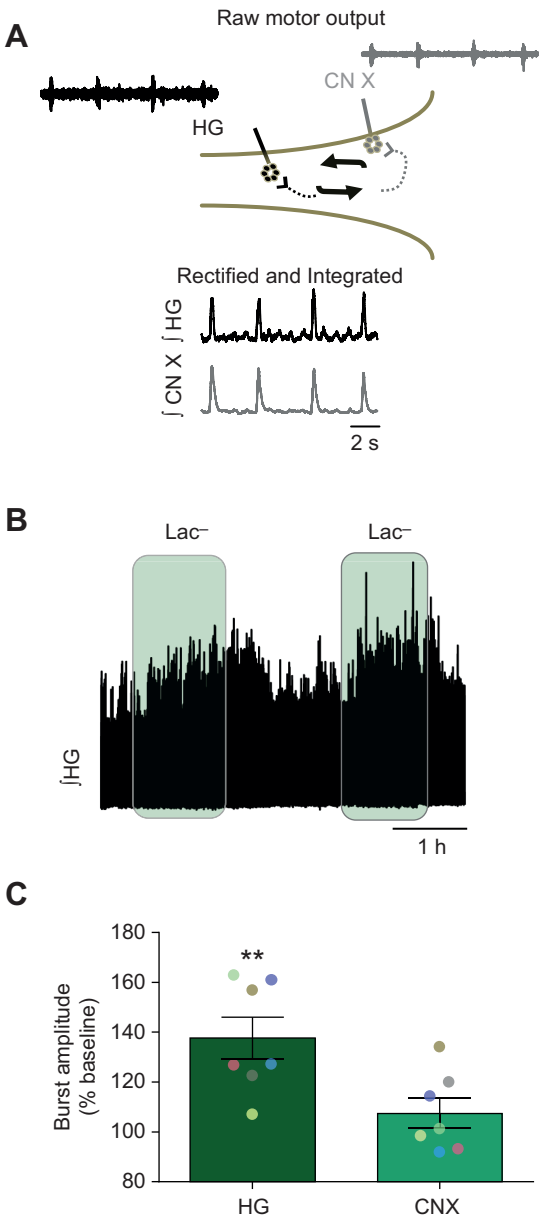

Fig. 1. Lactate increases respiratory-related motor output. (A) Simplified schematic diagram of the brainstem–spinal cord preparation. Raw signals from extracellular recordings are rectified and integrated for analysis. Large-amplitude signals that occur near-synchronously on both the hypoglossal (HG) and vagus (cranial X, CN X) nerve represent activity associated with lung breaths, while small-amplitude signals only for the HG represent neural activity with ventilation of the buccal cavity. (B) Compressed neurogram from the HG during exposure to 1 mmol l^{-1} lactate (Lac^-) for 1 h (green shaded area). In this example, lactate was washed from the preparation. Activity returned to near-baseline levels and the preparation was then re-exposed to lactate and washed again. (C) Mean (±s.e.m.; n=7) data showing change in burst amplitude of the lung burst on HG and CN X during 1 h exposure to 1 mmol l^{-1} lactate. Individual data points are from a single brainstem–spinal cord preparation, and like colors represent data taken from a single preparation. **P<0.01.

activation in the intact network. Resting membrane potential and firing frequency–current relationships were measured in current clamp. Series resistance and input resistance were measured in voltage clamp during a step from −80 mV to −70 mV, where series and input resistance were calculated using Ohm's law by measuring the peak transient and steady-steady currents, respectively. sEPCS were measured at −80 mV, sampled, and averaged in the 10 s period preceding the measurement of series and input resistance. Inward sEPSCs likely reflect AMPA glutamate receptor currents as we have described before in bullfrog vagal motor neurons (Santin et al., 2017), and also because −80 mV is below the activation threshold for the NMDA receptor and slightly positive to the estimated chloride Nernst potential. All physiological parameters were compared as the difference between the beginning and the end of the experiment for time control and lactate-exposed cells. We chose to assess the difference across the experimental time period to account for potential changes in neural properties over time, especially changes in synaptic properties known to occur during whole-cell patch clamp electrophysiology. Time control (n=7) and lactate-exposed neurons (n=7) were derived from 5 animals. For 6/7 neurons in each group, a time control and Lac^- experiment were run in the same slice, minimizing the potential for confounds associated with technical differences between time control and Lac^- groups. The resting membrane potential for neurons in time control experiments was −71.5±2.19 mV and that for lactate-exposed neurons was −70.4±2.19 mV (means±s.d.).

Data analysis

For series 1 experiments, the amplitude of the integrated nerve signals (peak amplitude minus baseline) and frequency of the HG and CN X activity were quantified for a 5 min baseline period, the last 5 min of the 1 h exposure to Lac^-, and after 1.5 h. In series 2 experiments, the amplitude of the integrated HG and CN X nerve signals was quantified for 3 min before exposure to Lac^-, HCO_3^- or Pyr^-, and in the last 3 min of each exposure. For whole-cell patch clamp experiments, membrane potential was recorded at the beginning and the end of the experiment. sEPSCs were sampled for 10 s in each treatment at the beginning and the end of the experiment (~200–400 events per cell). The high rate of sEPSCs in the slice is similar to values we obtained previously in vagal motor neurons (Santin et al., 2017). All data analysis was performed using LabChart software (ADInstruments).

Statistics

Parametric analyses were used when datasets passed normality tests and non-parametric analyses were used when they did not. Burst amplitude in series 1 experiments were analyzed using a two-tailed one-sample t-test to determine whether means were different from 100% (no change from baseline). Burst frequency in series 1 experiments was analyzed using a one-way ANOVA. Series 2 experiments were analyzed using a one-sample t-test to assess differences in burst amplitude from 100% (no change from baseline) after exposure to Lac^-, HCO_3^- and Pyr^-. We chose to analyze burst amplitude with one-sample t-tests because integrated extracellular amplitudes can vary across preparations based on the quality of the nerve, the seal of the electrode to the nerve, etc., and therefore can only be interpreted relatively (a change normalized to the internal baseline for each preparation); it is not appropriate to compare integrated nerve signals across preparations absolutely. Thus, the control amplitude must be 100% for each nerve and has no variance. As it is inappropriate to use an ANOVA when the control group has no variance, we used the two-tailed one-sample t-test to determine whether means were different from 100% and applied a Bonferroni correction to correct for multiple comparisons (i.e. we accepted the P-value as significant when P<0.017 for each of the three concentrations we tested). For whole-cell patch clamp electrophysiology experiments, we compared the difference between physiological properties at the beginning and end of the experiment

(membrane potential, firing properties, input resistance, sEPSC amplitude/frequency) in time control cells and cells exposed to 2 mmol l^{-1} sodium lactate to control for experimental effects of the whole-cell recording. Changes in membrane potential, input resistance, series resistance, sEPSC amplitude and sEPSC frequency were compared between control and Lac^- groups with two-tailed unpaired *t*-tests. Firing frequency–current input relationships (*F–I*) were compared at the beginning and end of the experiment using a two-way ANOVA. All analyses were performed using GraphPad Prism (v.6.01, San Diego, CA, USA). Significance was accepted when $P<0.05$.

RESULTS AND DISCUSSION

To identify a role for lactate in the central respiratory network, we isolated the brainstem–spinal cord from bullfrogs, *L. catesbeianus*. Fig. 1A shows rhythmic motor output recorded from two nerves: the hypoglossal nerve root (HG), which generates a large fraction of the drive to the buccal floor, and the vagus nerve, which plays a lesser role in activating the buccal pump but a major role in regulating airflow in and out of the lung by controlling the glottal dilator (CN X) (Sakakibara, 1983b). To assess sensitivity to lactate, we exposed preparations to 1 mmol l^{-1} sodium lactate (Lac^-) in the aCSF ($n=7$). We observed an increase in amplitude of HG output during exposure to Lac^- (Fig. 1B,C; 137.7±8.5% of baseline; $P=0.004$; one-sample *t*-test). These responses reversed upon washout (range 0.8–3.5 h) in all but one preparation (Fig. S1A). Lac^- did not significantly affect CN X amplitude (Fig. 1C; 107.6±5.9% of baseline; $P=0.248$; one sample *t*-test) or the frequency of respiratory bursts (Fig. S1B). Although Lac^- did not significantly affect CN X amplitude, some preparations did appear to respond, but the responses were more variable than those for HG from animal to animal. To internally confirm these results, we performed a separate series of experiments and applied Lac^- across a range of concentrations (0.5–4 mmol l^{-1}; $n=8$). Again, Lac^- increased output from HG at each concentration (0.5 and 2 mmol l^{-1}, $P<0.0001$ and 4 mmol l^{-1}, $P=0.0005$ compared with baseline with one-sample *t*-test) but did not significantly affect CN X amplitude (Fig. 2A). Thus, Lac^- stimulates motor output from the respiratory network, with specificity for motor outflow that activates inspiratory pump muscles of the buccal floor.

Sodium lactate is a base and raises aCSF pH by ∼0.02–0.1 units in this dose–response experiment. To control for small increases in pH, we increased pH to a similar extent by exposing the preparation to a different base, sodium bicarbonate (HCO_3^-), instead of Lac^- ($n=6$). These experiments not only control for slight increases in extracellular pH that could affect motor output but also control for slight increases in [Na^+], osmolality and stability of the motor amplitude of the preparation across time. HCO_3^- did not affect the amplitude of HG or CN X (Fig. 2B), demonstrating sensitivity to lactate rather than alkaline extracellular pH and several technical alternatives.

Lactate can also affect neuronal activity through changes in metabolism, intracellular pH and various non-metabolic effects on electrophysiological properties. To influence metabolism and intracellular pH, lactate enters cells through proton-coupled monocarboxylate transporters (MCTs). Lactate dehydrogenase then converts lactate to pyruvate for entry into the Krebs cycle, and the co-transported proton acidifies intracellular pH (Magistretti and Allaman, 2018). Like lactate, pyruvate is also a monocarboxylate that undergoes proton-coupled transport into cells via MCTs (Halestrap, 2011). To determine whether changes in pyruvate and/or the ensuing intracellular acidification during lactate superfusion increases motor output, we exposed preparations to sodium pyruvate, a common approach to identify metabolic versus non-metabolic effects of lactate (Thomsen et al., 2019; Yang et al., 2014). Unlike with lactate, HG and CN X activity did not change during pyruvate exposure over a range of doses (Fig. 2C). Collectively, these results argue for a direct excitatory action of lactate anions in the central respiratory network.

The previous experiments identified sensitivity of the respiratory motor outflow to lactate ions. Does lactate act directly at the level of the motor neuron, and what cellular processes does it target? To address this issue, we tested whether lactate enhances the excitatory drive of HG motor neurons — the individual neurons that comprise the nerve root that responded to lactate in our previous experiments. Using whole-cell patch clamp electrophysiology, we measured passive membrane properties, intrinsic excitability and excitatory postsynaptic activity in identified HG motor neurons in brainstem slices (Fig. 3A). As cellular functions often depend on cytosolic factors that are diluted during whole-cell recording, neurophysiological properties can change over the experimental time course. Thus, to account for time effects, we compared the change in properties from the beginning to the end of the experiment in slices superfused with either aCSF alone (time controls) or aCSF containing 2 mmol l^{-1} sodium lactate for 25 min. Exposure to 2 mmol l^{-1} lactate for 25 min did not affect firing rate, membrane potential or membrane input resistance relative to time controls (Fig. S2A–D). To assess synaptic function, we measured the amplitude and frequency of sEPSCs of HG motor neurons. In contrast to its effect on firing properties, lactate potentiated the mean amplitude of sEPSCs relative to time controls (Fig. 3B,C; $P=0.0006$; two-tailed unpaired *t*-test) but did not affect the frequency (Fig. 3D). In control experiments, we observed that the synaptic amplitude dropped over time (Fig. 3B,C), emphasizing the importance of time control experiments to detect changes in synaptic function, similar to that used to assess long-term potentiation with whole-cell patch clamp (Kato et al., 1993). Rundown of sEPSC amplitude was not caused by increases in series resistance or decreases in membrane input resistance because these variables did not change during the experiment (Fig. S3D,E). Taken together, our data strongly imply that lactate ions enhance the postsynaptic strength of motor neurons to increase respiratory motor outflow from the CNS.

Historically, physiologists have focused on how CO_2/pH in the brain and O_2 in the arterial blood regulate breathing. However, interest in the control of breathing by lactate in the arterial blood has undergone a resurgence (Chang et al., 2015; Thomsen et al., 2019, 2017), and the possibility that metabolites released in the brain during hypoxia, mainly ATP, has gained traction as an important mechanism for the control of ventilation (Angelova et al., 2015; Cinelli et al., 2017; Rajani et al., 2018). Furthermore, lactate stimulates catecholaminergic neurons in the brainstem to regulate cardiovascular parameters in mammals (Marina et al., 2015; Tang et al., 2014) and is involved in regulating body temperature in anuran amphibians (Branco and Steiner, 1999). As lactate is known to rise in the CNS during challenges to respiratory homeostasis across vertebrates (e.g. Bandurski et al., 1968; Marina et al., 2015; Matsui et al., 2017), we tested the hypothesis that lactate ions directly stimulate the respiratory network using an amphibian model.

We found that low concentrations of lactate increased hypoglossal motor output that contributes to buccal pump activation in anuran amphibians (Kogo et al., 1994; West and Jones, 1975). However, lactate did not affect the frequency of respiratory-related activity or vagal motor output that predominately activates glottal muscular which gates lung airflow. Although lactate transport between astrocytes and neurons can influence ventilation through pH (Erlichman et al., 2008), increases in motor output do not likely involve changes in pH as raising extracellular pH and pyruvate did

Journal of Experimental Biology (2020) 223, jeb235705. doi:10.1242/jeb.235705

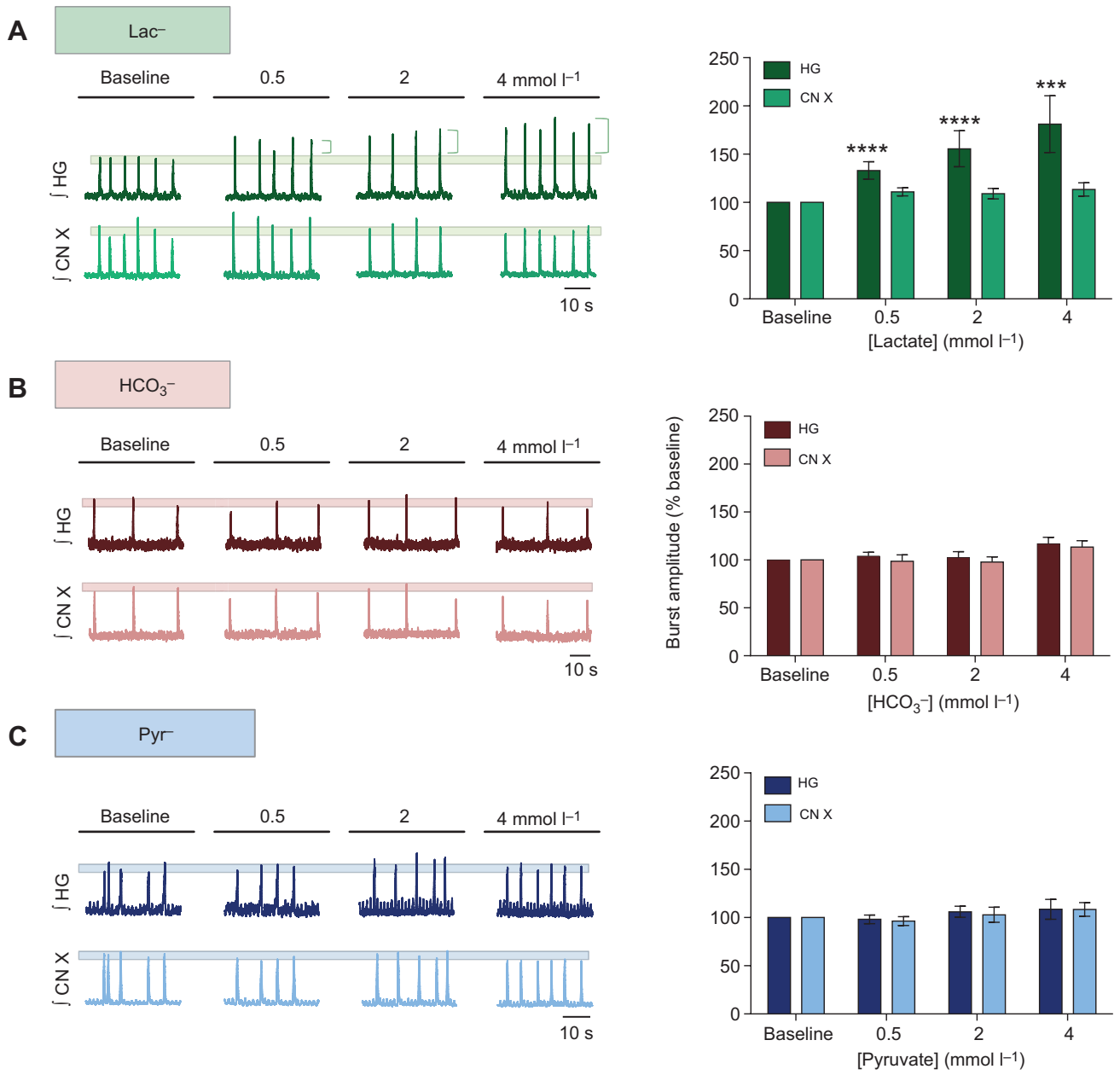

Fig. 2. pH and pyruvate do not account for increases in HG output induced by lactate. (A) Left: example recording of HG and CN X activity from a dose–response experiment with 0.5, 2 and 4 mmol l^{-1} lactate. Mean (±s.e.m.; *n*=8) data are shown in the bar graph on the right. HG activity at each dose is significantly different from 100% (***P<0.0005, ****P<0.0001). (B) Left: example recording of HG and CN X activity during exposure to 0.5, 2 and 4 mmol l^{-1} sodium bicarbonate (HCO_3^-). Mean (±s.e.m.; *n*=6) data are shown on the right. (C) Left: example recording of HG and CN X activity during exposure to 0.5, 2 and 4 mmol l^{-1} pyruvate. Mean (±s.e.m.; *n*=6) data are shown on the right.

not elicit similar motor responses to those with lactate (Fig. 2B,C). These results suggest pH and metabolic-independent effects of lactate on motor drive to the buccal floor. As increased motor output that controls the buccal pump corresponds with greater lung inflation volume in amphibians (Sakakibara, 1983a), we suggest that lactate sensitivity may contribute to enhanced ventilation during bouts of high respiratory demand when lactate increases in the CNS. These results are especially intriguing because lactate increases ventilation through changes in tidal volume in rats (Gargaglioni et al., 2003; Hardarson et al., 1998). Although regulation of tidal volume is complex, these results suggest that lactate may contribute to increases in tidal volume during metabolic challenges through conserved actions on motor neurons.

What sources of lactate may activate hypoglossal motor output, and what mechanisms transduce it? During a metabolic disturbance, lactate from several sources could elicit this response. For example, circulating lactate may cross the blood–brain barrier (Halestrap, 2011), astrocytes may release lactate into the interstitial space (Matsui et al., 2017; Newman et al., 2011), or lactate may be derived intrinsically from HG motor neurons during hypoxia. Several possible mechanisms could then account for neuronal responses to lactate, including membrane depolarization (Marina et al., 2015; Sada et al., 2015), increased firing rates (Tang et al., 2014) and modified synaptic transmission (de Castro Abrantes et al., 2019; Yang et al., 2014). Of these possibilities, we found that lactate increased the amplitude of excitatory postsynaptic currents of HG

Journal of Experimental Biology (2020) 223, jeb235705. doi:10.1242/jeb.235705

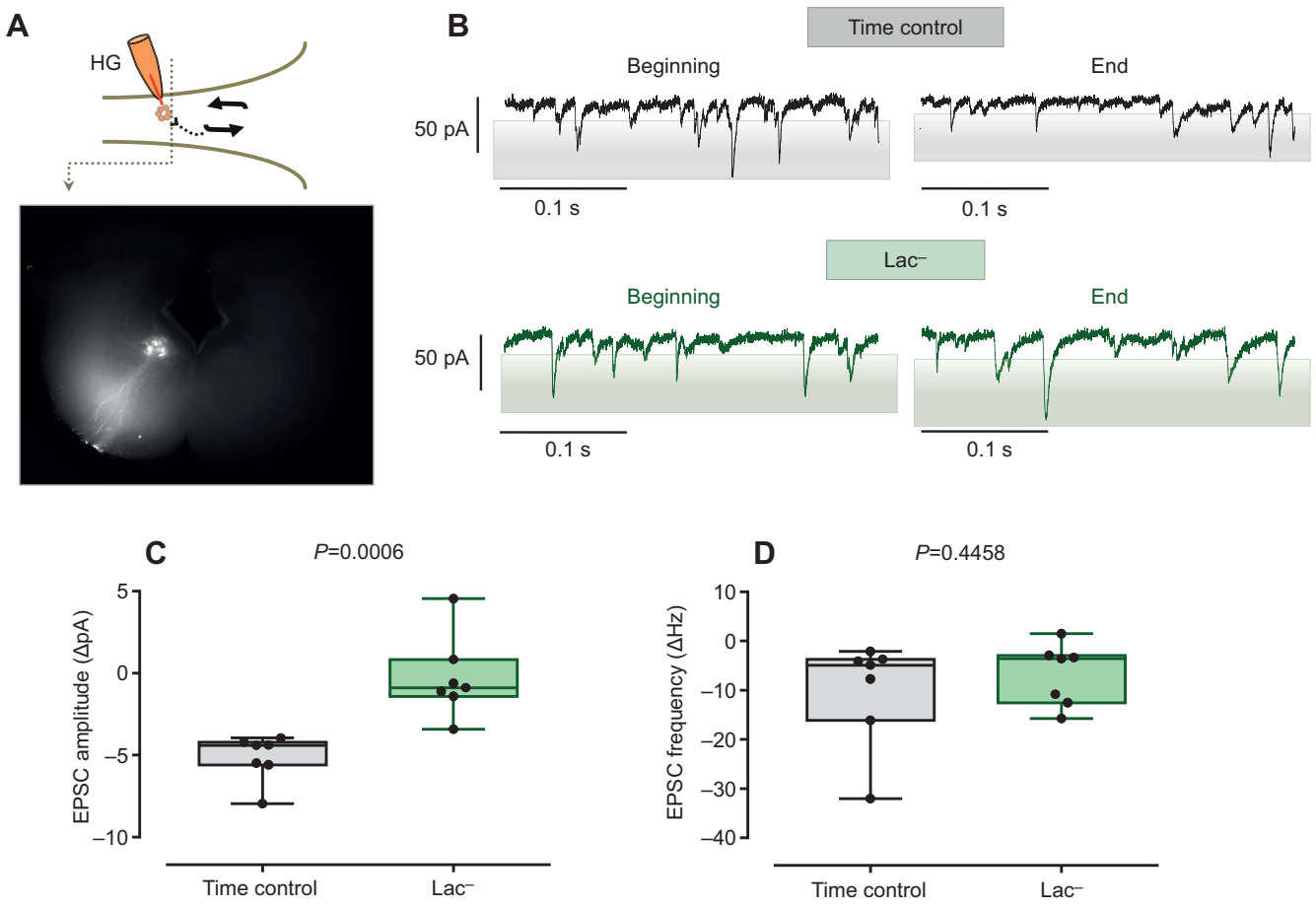

Fig. 3. Lactate potentiates excitatory synaptic strength of HG motor neurons. (A) Fluorescence labeling with TRITC dextran indicates neurons backfilled through HG in the rostral part of the nucleus. (B) Example recordings of spontaneous excitatory postsynaptic currents (sEPSCs) at the beginning (i.e. baseline) and end of the 25 min recording period (top, aCSF time control; bottom, 2 mmol l^{-1} lactate treatment). (C) Mean data (absolute change in amplitude from baseline) showing that lactate potentiates the mean sEPSC amplitude relative to time controls (n=7 neurons per group). (D) Mean data (absolute change in frequency from baseline) showing that lactate did not influence sESPC frequency relative to time controls. Whiskers show the maximum and minimum; circles represent individual data points.

motor neurons, which is likely to amplify postsynaptic responses to presynaptic rhythm generating input to elevate motor output in the intact network. Increases in the amplitude of postsynaptic currents suggests that lactate influences neurotransmitter receptors or the amount of neurotransmitter released into the synaptic cleft, as these variables account for variation in spontaneous postsynaptic current amplitude (Liu et al., 1999). The signaling processes that link lactate to synaptic strength in respiratory motor neurons are not yet known; however, lactate initiates second messenger signaling cascades through G-protein coupled receptors (Chang et al., 2015; de Castro Abrantes et al., 2019; Tang et al., 2014) that may modulate synaptic receptors. Additionally, lactate can influence redox status to enhance NMDA-glutamate currents to rapidly increase the expression of genes involved in synaptic plasticity (Yang et al., 2014). Therefore, several possible intracellular and extracellular molecular mechanisms may link variations in lactate to synaptic strength.

Overall, our results present a mechanism whereby lactate ions in the CNS couple respiratory drive to metabolic demands through actions on motor neurons. It remains to be determined whether lactate acts on other network components, such as glia and neuromodulatory regions, and how these processes operate *in vivo*. As many general features of the respiratory network are shared across vertebrates (Kinkead, 2009; Ramirez et al., 2016), a central lactate sensor may represent a conserved trait for the control of breathing. Animals within and across species have a wide range of respiratory demands due to their ecological niche, lifestyle and evolutionary history (Santin, 2018). Thus, insights that build upon this finding will undoubtedly come from the study of species and contexts where lactate accumulates in the CNS. In conclusion, these results introduce the possibility that lactate ions in the CNS regulate output from the respiratory network.

Acknowledgements
We would like to thank Lynn Hartzler for comments on a draft of the manuscript and for conversations about the implications of these data.

Competing interests
The authors declare no competing or financial interests.

Author contributions
Conceptualization: J.M.S.; Formal analysis: J.M.S.; Investigation: M.T.B., J.M.S.; Data curation: M.T.B., J.M.S.; Writing - original draft: J.M.S.; Writing - review & editing: J.M.S.; Visualization: J.M.S.; Supervision: J.M.S.; Project administration: J.M.S.; Funding acquisition: J.M.S.

Funding
This work was funded in part by a grant from the National Institutes of Health (R15NS112920), as well as laboratory startup funds from the University of North Carolina at Greensboro to J.M.S. Deposited in PMC for release after 12 months.

Supplementary information

Supplementary information available online at
https://jeb.biologists.org/lookup/doi/10.1242/jeb.235705.supplemental

References

Angelova, P. R., Kasymov, V., Christie, I., Sheikhbahaei, S., Turovsky, E., Marina, N., Korsak, A., Zwicker, J., Teschemacher, A. G., Ackland, G. L. et al. (2015). Functional oxygen sensitivity of astrocytes. *J. Neurosci.* **35**, 10460-10473. doi:10.1523/JNEUROSCI.0045-15.2015

Baghdadwala, M. I., Duchcherer, M., Trask, W. M., Gray, P. A. and Wilson, R. J. A. (2016). Diving into the mammalian swamp of respiratory rhythm generation with the bullfrog. *Respir. Physiol. Neurobiol.* **224**, 37-51. doi:10.1016/j.resp.2015.09.005

Bandurski, R. S., Bradstreet, E. and Scholander, P. F. (1968). Metabolic changes in the mud-skipper during asphyxia or exercise. *Comp. Biochem. Physiol.* **24**, 271-274. doi:10.1016/0010-406X(68)90974-2

Bergersen, L. H. (2015). Lactate transport and signaling in the brain: potential therapeutic targets and roles in body—Brain interaction. *J. Cereb. Blood Flow Metab.* **35**, 176-185. doi:10.1038/jcbfm.2014.206

Bisgard, G. E., Forster, H. V., Byrnes, B., Stanek, K., Klein, J. and Manohar, M. (1978). Cerebrospinal fluid acid-base balance during muscular exercise. *J. Appl. Physiol.* **45**, 94-101. doi:10.1152/jappl.1978.45.1.94

Branco, L. G. S. and Steiner, A. A. (1999). Central thermoregulatory effects of lactate in the toad Bufo paracnemis. *Comp. Biochem. Physiol. A Mol. Integr. Physiol.* **122**, 457-461. doi:10.1016/S1095-6433(99)00032-X

Chang, A. J., Ortega, F. E., Riegler, J., Madison, D. V. and Krasnow, M. A. (2015). Oxygen regulation of breathing through an olfactory receptor activated by lactate. *Nature* **527**, 240. doi:10.1038/nature15721

Chang, A. J., Kim, N. S., Hireed, H., de Arce, A. D., Ortega, F. E., Riegler, J., Madison, D. V. and Krasnow, M. A. (2018). Chang et al. reply. *Nature* **561**, E41. doi:10.1038/s41586-018-0547-7

Cinelli, E., Iovino, L. and Mutolo, D. (2017). ATP and astrocytes play a prominent role in the control of the respiratory pattern generator in the lamprey. *J. Physiol.* **595**, 7063-7079. doi:10.1113/JP274749

de Castro Abrantes, H., Briquet, M., Schmuziger, C., Restivo, L., Puyal, J., Rosenberg, N., Rocher, A.-B., Offermanns, S. and Chatton, J.-Y. (2019). The lactate receptor HCAR1 modulates neuronal network activity through the activation of Gα and Gβγ subunits. *J. Neurosci.* **39**, 4422-4433. doi:10.1523/JNEUROSCI.2092-18.2019

Erlichman, J. S., Hewitt, A., Damon, T. L., Hart, M., Kurascz, J., Li, A. and Leiter, J. C. (2008). Inhibition of monocarboxylate transporter 2 in the retrotrapezoid nucleus in rats: a test of the astrocyte–neuron lactate-shuttle hypothesis. *J. Neurosci.* **28**, 4888-4896. doi:10.1523/JNEUROSCI.5430-07.2008

Gargaglioni, L. H., Bicego, K. C., Steiner, A. A. and Branco, L. G. S. (2003). Lactate as a modulator of hypoxia-induced hyperventilation. *Respir. Physiol. Neurobiol.* **138**, 37-44. doi:10.1016/S1569-9048(03)00172-1

Gourine, A. V., Kasymov, V., Marina, N., Tang, F., Figueiredo, M. F., Lane, S., Teschemacher, A. G., Spyer, K. M., Deisseroth, K. and Kasparov, S. (2010). Astrocytes control breathing through pH-dependent release of ATP. *Science* **329**, 571-575. doi:10.1126/science.1190721

Guyenet, P. G. and Bayliss, D. A. (2015). Neural control of breathing and CO_2 homeostasis. *Neuron* **87**, 946-961. doi:10.1016/j.neuron.2015.08.001

Halestrap, A. P. (2011). Monocarboxylic acid transport. *Comprehens. Physiol.* **3**, 1611-1643. doi:10.1002/cphy.c130008

Hardarson, T., Skarphedinsson, J. O. and Sveinsson, T. (1998). Importance of the lactate anion in control of breathing. *J. Appl. Physiol.* **84**, 411-416. doi:10.1152/jappl.1998.84.2.411

Kato, K., Clifford, D. B. and Zorumski, C. F. (1993). Long-term potentiation during whole-cell recording in rat hippocampal slices. *Neuroscience* **53**, 39-47. doi:10.1016/0306-4522(93)90282-K

Kinkead, R. (2009). Phylogenetic trends in respiratory rhythmogenesis: insights from ectothermic vertebrates. *Respir. Physiol. Neurobiol.* **168**, 39-48. doi:10.1016/j.resp.2009.05.011

Kogo, N. and Remmers, J. E. (1994). Neural organization of the ventilatory activity in the frog, *Rana catesbeiana*. II. *J. Neurobiol.* **25**, 1080-1094. doi:10.1002/neu.480250905

Kogo, N., Perry, S. F. and Remmers, J. E. (1994). Neural organization of the ventilatory activity in the frog, *Rana catesbeiana*. I. *J. Neurobiol.* **25**, 1067-1079. doi:10.1002/neu.480250904

Liu, G., Choi, S. and Tsien, R. W. (1999). Variability of neurotransmitter concentration and nonsaturation of postsynaptic AMPA receptors at synapses in hippocampal cultures and slices. *Neuron* **22**, 395-409. doi:10.1016/S0896-6273(00)81099-5

Magistretti, P. J. and Allaman, I. (2018). Lactate in the brain: from metabolic end-product to signalling molecule. *Nat. Rev. Neurosci.* **19**, 235-249. doi:10.1038/nrn.2018.19

Marina, N., Ang, R., Machhada, A., Kasymov, V., Karagiannis, A., Hosford, P. S., Mosienko, V., Teschemacher, A. G., Vihko, P., Paton, J. F. R. et al. (2015). Brainstem hypoxia contributes to the development of hypertension in the spontaneously hypertensive rat. *Hypertension* **65**, 775-783. doi:10.1161/HYPERTENSIONAHA.114.04683

Matsui, T., Omuro, H., Liu, Y.-F., Soya, M., Shima, T., McEwen, B. S. and Soya, H. (2017). Astrocytic glycogen-derived lactate fuels the brain during exhaustive exercise to maintain endurance capacity. *Proc. Natl Acad. Sci. USA* **114**, 6358-6363. doi:10.1073/pnas.1702739114

Newman, L. A., Korol, D. L. and Gold, P. E. (2011). Lactate produced by glycogenolysis in astrocytes regulates memory processing. *PLoS ONE* **6**, e28427. doi:10.1371/journal.pone.0028427

Peng, Y.-J., Gridina, A., Wang, B., Nanduri, J., Fox, A. P. and Prabhakar, N. R. (2020). Olfactory receptor 78 participates in carotid body response to a wide range of low O_2 levels but not severe hypoxia. *J. Neurophysiol.* **123**, 1886-1895. doi:10.1152/jn.00075.2020

Rajani, V., Zhang, Y., Jalubula, V., Rancic, V., Sheikhbahaei, S., Zwicker, J. D., Pagliardini, S., Dickson, C. T., Ballanyi, K., Kasparov, S. et al. (2018). Release of ATP by pre-Bötzinger complex astrocytes contributes to the hypoxic ventilatory response via a Ca^{2+}-dependent P2Y1 receptor mechanism. *J. Physiol.* **596**, 3245-3269. doi:10.1113/JP274727

Ramirez, J.-M., Dashevskiy, T., Marlin, I. A. and Baertsch, N. (2016). Microcircuits in respiratory rhythm generation: commonalities with other rhythm generating networks and evolutionary perspectives. *Curr. Opin. Neurobiol.* **41**, 53-61. doi:10.1016/j.conb.2016.08.003

Sada, N., Lee, S., Katsu, T., Otsuki, T. and Inoue, T. (2015). Targeting LDH enzymes with a stiripentol analog to treat epilepsy. *Science* **347**, 1362-1367. doi:10.1126/science.aaa1299

Sakakibara, Y. (1983a). The pattern of respiratory nerve activity in the bullfrog. *Jpn. J. Physiol.* **34**, 269-282. doi:10.2170/jjphysiol.34.269

Sakakibara, Y. (1983b). Trigeminal nerve activity and buccal pressure as an index of total inspiratory activity in the bullfrog. *Jpn. J. Physiol.* **34**, 827-838. doi:10.2170/jjphysiol.34.827

Santin, J. M. (2018). How important is the CO_2 chemoreflex for the control of breathing? Environmental and evolutionary considerations. *Comp. Biochem. Physiol. A Mol. Integr. Physiol.* **215**, 6-19. doi:10.1016/j.cbpa.2017.09.015

Santin, J. M., Vallejo, M. and Hartzler, L. K. (2017). Synaptic up-scaling preserves motor circuit output after chronic, natural inactivity. *eLife* **6**, e30005. doi:10.7554/eLife.30005

Takei, K., Oka, Y., Satou, M. and Ueda, K. (1987). Distribution of motoneurons involved in the prey-catching behavior in the Japanese toad, *Bufo japonicus*. *Brain Res.* **410**, 395-400. doi:10.1016/0006-8993(87)90346-5

Tang, F., Lane, S., Korsak, A., Paton, J. F. R., Gourine, A. V., Kasparov, S. and Teschemacher, A. G. (2014). Lactate-mediated glia-neuronal signalling in the mammalian brain. *Nat. Commun.* **5**, 3284. doi:10.1038/ncomms4284

Thomsen, M. T., Wang, T., Milsom, W. K. and Bayley, M. (2017). Lactate provides a strong pH-independent ventilatory signal in the facultative air-breathing teleost *Pangasianodon hypophthalmus*. *Sci. Rep.* **7**, 6378. doi:10.1038/s41598-017-06745-4

Thomsen, M. T., Lefevre, S., Nilsson, G. E., Wang, T. and Bayley, M. (2019). Effects of lactate ions on the cardiorespiratory system in rainbow trout (Oncorhynchus mykiss). *Am. J. Physiol. Regul. Integr. Comp. Physiol.* **316**, R607-R620. doi:10.1152/ajpregu.00395.2018

Torres-Torrelo, H., Ortega-Sáenz, P., Macías, D., Omura, M., Zhou, T., Matsunami, H., Johnson, R. S., Mombaerts, P. and López-Barneo, J. (2018). The role of Olfr78 in the breathing circuit of mice. *Nature* **561**, E33. doi:10.1038/s41586-018-0545-9

West, N. H. and Jones, D. R. (1975). Breathing movements in the frog *Rana pipiens*. I. The mechanical events associated with lung and buccal ventilation. *Can. J. Zool.* **53**, 332-344. doi:10.1139/z75-042

Yang, J., Ruchti, E., Petit, J.-M., Jourdain, P., Grenningloh, G., Allaman, I. and Magistretti, P. J. (2014). Lactate promotes plasticity gene expression by potentiating NMDA signaling in neurons. *Proc. Natl Acad. Sci. USA* **111**, 12228-12233. doi:10.1073/pnas.1322912111

Supplementary Information

Fig. S1.

Burst amplitude returns to near-baseline levels in 6/7 preparations following washout of lactate. (A) In the 6 preparations that returned to near-control burst amplitude, recovery time ranged from 0.8-3.5 hrs. (B) The Frequency of respiratory motor output was not significantly affected by lactate (p=0.1556, paired t test).

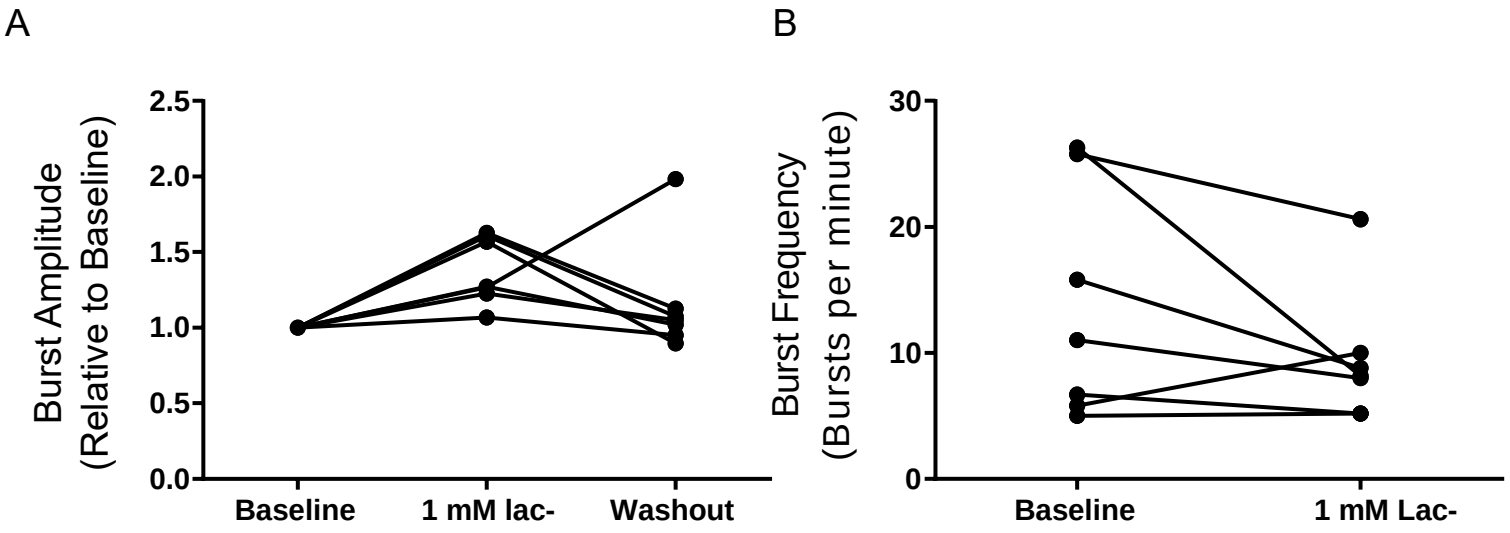

Fig. S2.

Lactate does not affect firing responses and membrane properties of hypoglossal motor neurons. (A) shows firing rates at baseline and then after 25 minutes of whole-cell patch clamp recording in response to step increases in current. (B) shows firing rates before and after exposure to 2 mM lactate. (C-E) show that membrane potential, input resistance, and series resistance does not differ between time control neurons and those exposed lactate for 25 minutes.